



**Radar observations
of an orographic
precipitation event**

M. Frech and J. Steinert

This discussion paper is/has been under review for the journal Hydrology and Earth System Sciences (HESS). Please refer to the corresponding final paper in HESS if available.

Polarimetric radar observations during an orographic rain event and the performance of a hydrometeor classification scheme

M. Frech¹ and J. Steinert²

¹DWD, German Meteorological Service, Meteorologisches Observatorium Hohenpeißenberg, Albin-Schwaiger-Weg 10, 82383 Hohenpeißenberg, Germany

²DWD, German Meteorological Service, Frankfurter Str. 135, 63067 Offenbach am Main, Germany

Received: 4 July 2014 – Accepted: 15 July 2014 – Published: 29 July 2014

Correspondence to: M. Frech (michael.frech@dwd.de)

Published by Copernicus Publications on behalf of the European Geosciences Union.

Title Page

Abstract Introduction

Conclusions References

Tables Figures

⏪ ⏩

◀ ▶

Back Close

Full Screen / Esc

Printer-friendly Version

Interactive Discussion



Abstract

An intense orographic precipitation event is analysed using two polarimetric C-Band radars situated north of the Alps on 5 January 2013. One radar is operated at DWD's meteorological observatory Hohenpeißenberg (MHP, 1006 m a.s.l. – above sea level) and the Memmingen (MEM, 65 km west of MHP, 600 m a.s.l.) radar is part of DWD's operational radar network. The event lasted about 1.5 days and in total 44 mm precipitation was measured at Hohenpeißenberg. Detailed high resolution observation on the vertical structure of this event is obtained through a birdbath scan at 90° elevation which is part of the operational scanning. This scan is acquired every 5 min and provides meteorological profiles at high spatial resolution. In the course of this event, the melting layer (ML) descends until the transition from rain into snow is observed at ground level. This transition from rain into snow is well documented by local weather observers and a present-weather sensor. The orographic precipitation event reveals mesoscale variability above the melting layer which is unexpected from a meteorological point of view. It corresponds to a substantial increase in rain rate at the surface. The performance of the newly developed hydrometeor classification scheme "Hymec" using Memmingen radar data over Hohenpeißenberg is analyzed. The detection in location and timing of the ML agrees well with the Hohenpeißenberg radar data. Considering the size of the Memmingen radar sensing volume, the detected hydrometeor (HM) types are consistent for measurements at or in a ML, even though surface observation indicate for example rain whereas the predominant HM is classified as wet snow. To better link the HM classification with the surface observation, either better thermodynamic input is needed for Hymec or a statistical correction of the HM classification similar to a model output statistics (MOS) approach may be needed.

HESSD

11, 8845–8877, 2014

Radar observations of an orographic precipitation event

M. Frech and J. Steinert

[Title Page](#)

[Abstract](#)

[Introduction](#)

[Conclusions](#)

[References](#)

[Tables](#)

[Figures](#)



[Back](#)

[Close](#)

[Full Screen / Esc](#)

[Printer-friendly Version](#)

[Interactive Discussion](#)



1 Introduction

Orographic rain events in the vicinity of the Alps can last a couple of days and often have the potential to produce flooding conditions. The Alps represent a natural barrier for advected moist air which either initiates or intensifies the precipitation process. The precipitation events are often persistent and depending on the season, transitions from rain into snow caused by diabatic cooling of the associated airmass can be observed (Lackmann et al., 2002). From an operational point of view, precipitation amount and hydrometeor type are important parameters which are needed to issue proper warnings to the public. For example, correct precipitation amounts are important for flood management. The correct hydrometeor classification is an important parameter for the traffic management. Here, modern radar systems are the only systems which are able to provide spatial informations about the meteorological situation associated with a sufficient update rate (Scharfenberg et al., 2005). This is one reason, why the German meteorological service DWD is running a weather radar network which is currently undergoing a major upgrade. The new generation of radar systems of the German weather radar network is fully polarized. The systems are run in a hybrid (STAR) mode, simultaneous transmitting in horizontal and vertical polarization (see Frech et al., 2013, for some more technical details of the new system). The scan strategy guarantees an update rate of 5 min. It comprises a terrain following scan (the so called precipitation scan), a 5 min volume with 10 sweeps at 10 different elevations and a “birdbath” scan at 90° elevation. Latter scan is part of the scan strategy because of the necessity to calibrate differential moments such as the differential reflectivity ZDR. The differential reflectivity of falling hydrometeors must be zero when looking vertically upward. Hardware specific offsets can be derived and monitored using this scan. The offsets are used to correct the differential reflectivity data. This scan can also be used to monitor the absolute calibration of the radar system (Frech, 2013). Aside from this, the birdbath scan can be viewed as a profiler scan and is as such a very interesting scan from a meteorological point of view. Typically this scan is not used operationally for this purpose

HESSD

11, 8845–8877, 2014

Radar observations of an orographic precipitation event

M. Frech and J. Steinert

[Title Page](#)

[Abstract](#)

[Introduction](#)

[Conclusions](#)

[References](#)

[Tables](#)

[Figures](#)



[Back](#)

[Close](#)

[Full Screen / Esc](#)

[Printer-friendly Version](#)

[Interactive Discussion](#)



so far. The birdbath scan provides a high resolution look of the precipitation process above the radar site. This will be highlighted in this paper.

In this work we use data from the research radar at DWD's meteorological observatory Hohenpeißenberg (MHP, 1006 m a.s.l.) and the Memmingen radar (MEM, 65 km west of MHP, 600 m a.s.l.) which is part of DWD's operational radar network. Both systems are of the same type. For this work, the configuration of the research radar was identical to the Memmingen system. In general, the research system does not provide operational data.

The introduction of the new dual-polarization radar system was accompanied by a project called "Radarmaßnahmen". This inhouse DWD project covers the development of radar data processing algorithms, e.g. for quality assurance, hydrometeor classification and quantitative precipitation estimation and the development of a software framework which is called "POLARA" (Polarimetric Radar Algorithms; Rathmann and Mott, 2012). Currently the aforementioned algorithms within the POLARA framework are in a pre-operational verification test phase. The software package is planned to become operational in 2014.

The principal physical processes of precipitation are well known but with the availability of new technology often a closer and also new look into the precipitation process becomes possible, especially when new methods and algorithms such as a hydrometeor classification move from the research world to the operational world of a weather service, simply because more observations become available.

In this paper we analyze an orographic precipitation event and verify the performance of the hydrometeor classification scheme. The analysis focuses on the mesoscale variability of the precipitation event. We first introduce hydrometeor classification scheme before we analyze the features of the precipitation event using radar data and surface observations. The analysis is then used to verify the classification scheme. The main findings are summarized in the last section.

HESSD

11, 8845–8877, 2014

Radar observations of an orographic precipitation event

M. Frech and J. Steinert

[Title Page](#)

[Abstract](#)

[Introduction](#)

[Conclusions](#)

[References](#)

[Tables](#)

[Figures](#)

[⏪](#)

[⏩](#)

[⏴](#)

[⏵](#)

[Back](#)

[Close](#)

[Full Screen / Esc](#)

[Printer-friendly Version](#)

[Interactive Discussion](#)



2 Hydrometeor classification

The additional polarimetric measurements of a dual-polarization radar allows the classification of the hydrometeor type in the pulse volume. Methodologies to classify hydrometeors using polarimetric radar data are described for example by Straka et al. (2000), Keenan (2003) and Lim et al. (2005). Based on these results, weather services, like the National Weather Service (NWS) of the USA or Météo-France, started to implement suitable hydrometeor classification schemes. Related publications are Park et al. (2009) for the American algorithm and Al-Sakka et al. (2013) for the French scheme. Both versions use a fuzzy logic classification with a comparable set of input parameters and estimated hydrometeor classes. The verification of a classification schemes is typically done with test data sets, where hydrometeor types are known (Al-Sakka et al., 2013). Radar derived classification results can be related to surface observation by using model derived thermodynamic profiles (Schuur et al., 2012). The biggest challenge is a situation with mixed precipitation where a pure objective validation is usually not possible.

At DWD, we implemented a fuzzy logic hydrometeor classification algorithm (Hymec) which follows Park et al. (2009). The algorithm is currently in the evaluation and verification phase. A brief overview on the Hymec algorithm implementation is given in the following.

Initially we decided on the set hydrometeor classes to be covered by Hymec based on a user survey. There, the request for a light rain class (drizzle) should be mentioned owing to long lasting drizzle events over Germany. We then harmonized the requested list of hydrometeor classes with classification algorithms that are available based on literature focusing on the work of Park et al. (2009). The following classes are considered by Hymec: drizzle (DR), raindrops (RA), big drops (BD), wet snowflakes (WS), dry snowflakes (DS), ice crystals (IC), graupel (GR), heavy rain or hail stones (RH) and hail stones (HA). In addition, the melting layer (ML; bright band) represents a class on its own. In the Hymec algorithm chain the melting layer detection is done prior the

HESSD

11, 8845–8877, 2014

Radar observations of an orographic precipitation event

M. Frech and J. Steinert

Title Page

Abstract

Introduction

Conclusions

References

Tables

Figures



Back

Close

Full Screen / Esc

Printer-friendly Version

Interactive Discussion



hydrometeor classification. We use the ML detection as an additional source of information which is offered to the user to interpret the meteorological situation. Algorithms like the quantitative precipitation estimation (QPE) use the knowledge of the ML location and the type of hydrometeor to utilize appropriate precipitation estimation algorithms.

5 The Hymec data processing chain

The input data for Hymec consists on the one hand of PPI radar data and on the other hand of output data from the NWP model COSMO-DE (Baldauf et al., 2014). From the pool of the dual-polarimetric measurements the reflectivity in horizontal channel Zh, the differential reflectivity ZDR, the specific differential phase KDP, the co-polarization correlation coefficient ρ_{hv} and the differential phase KDP are used. The radar moments have passed a quality control chain, where especially clutter segments and other non-meteorological artefacts in the radar data like spokes and rings are treated (Werner and Steinert, 2012). The correction of the path attenuation plays a major role in the quality assurance and is based on Zh and ZDR. As the attenuation correction algorithm needs homogeneous (related to hydrometeor class) ray segments, the results of a first Hymec run is used as input. There, the COSMO-DE model delivers the temperature related information in order to separate between liquid and solid hydrometeor types. Especially snow flakes and small raindrops give similar radar signatures. Without a temperature information it is difficult to distinguish those hydrometeor types. The two single level grid products of the height of the 0°C-isotherm, HZEROCL, and the snowfall height SNOWLMT are used. Furthermore, a history of the detected ML is created and is used as another input parameter. The ML history is created, because at low elevation angles the detection of the ML is difficult (Giangrande et al., 2008). A minor reason is the long path through a ML such that a clear ML signal may be blurred. A major reason is however, that the ML cannot be detected at low elevations, if the ML is situated above the radar sweep. Because of that the ML history is based on the ML detection of high elevation sweeps of the volume scan.

Radar observations of an orographic precipitation event

M. Frech and J. Steinert

[Title Page](#)

[Abstract](#)

[Introduction](#)

[Conclusions](#)

[References](#)

[Tables](#)

[Figures](#)



[Back](#)

[Close](#)

[Full Screen / Esc](#)

[Printer-friendly Version](#)

[Interactive Discussion](#)



Hymec is implemented as a two-stage algorithm sequence. A sketch of the embedded classification processing chain is shown in Fig. 1. The first run is placed in front of the attenuation path correction algorithm and the second run thereafter (Steinert et al., 2013). The final classification results are taken from the second run.

As mentioned before, the hydrometeor classification is connected with a prefix ML detection. In Fig. 2, the corresponding data paths between the ML detection and the hydrometeor classification are shown for the second run of Hymec.

The ML detection and the hydrometeor classification are both based on a fuzzy logic core. To allow a generic fuzzification, every input parameter must be projected such that it is consistent with radar data. Since NWP grid fields and ML history are initially not in radar-centric polar coordinates a polar data matrix is generated in a pre-processing step. The result is a polar data matrix for each radar site with the height information related to the height of the radar measurements in the dimension of the original radar data matrix.

The fuzzy logic method itself is based on trapezoidal membership functions (MBF) for each pair of input parameter and hydrometeor class. This means MBF for HZE-ROCL, SNOWLMT and the ML history have to be created. For the parameterization of the MBF for radar input the values of Park et al. (2009) are used as a first guess. If necessary, those MBF will be optimized based on verification results. The winner class of the fuzzy logic is estimated with the maximum method related to the class probability. Furthermore the class probability of the winner class have to exceed a threshold (35 % for the HM classes, and 65 % for the ML class). If the class probability is below the threshold, the class is “not classified” (NC).

After the utilization of the fuzzy logic scheme a post-processing part follows. There the ML detection is optimized and updated in order to improve the reliability of the resulting ML detection. Following steps are considered:

- combination of ML segments along the radar ray which seem to belong together,
- smoothing of the ML detection by using the detection in the neighboring rays and

HESSD

11, 8845–8877, 2014

Radar observations of an orographic precipitation event

M. Frech and J. Steinert

[Title Page](#)

[Abstract](#)

[Introduction](#)

[Conclusions](#)

[References](#)

[Tables](#)

[Figures](#)

[⏪](#)

[⏩](#)

[◀](#)

[▶](#)

[Back](#)

[Close](#)

[Full Screen / Esc](#)

[Printer-friendly Version](#)

[Interactive Discussion](#)



– update of the ML history for this time stamp.

3 The orographic precipitation event: surface and radar observations at Hohenpeißenberg

An intense orographic precipitation event was observed using two polarimetric C-Band radar situated 20–40 km north of the Alps on 5 January 2013. The event lasted about 1.5 days and in total 44 mm precipitation were measured at Hohenpeißenberg. Synoptically, Germany was located at the forefront stationary longwave ridge which extended from the Iberian Peninsula up to the British Isles. Embedded in the upper air-flow from NW–NNW a warm-front caused the intense and persistent orographic rain event especially in South-Eastern Bavaria.

We first analyze data from the birdbath scan in order to highlight the temporal evolution of this orographic precipitation event in detail. During Saturday (5 January 2013) a transition from rain into snow was observed. The Hohenpeißenberg weather observers noted sleet starting 14:40 UTC and pure snow fall beginning 16:45 UTC. Figure 3 is a time-height plot of the unfiltered reflectivity factor UZh starting 00:00 UTC, 5 January 2013, ending 03:00 UTC 6 January 2013. Unfiltered UZh means that no clutter filter has been applied. Only data above approximately 600 m above the radar site are shown, which approximately corresponds to the farfield of the radar antenna. Meaningful data is expected from this range on. From Fig. 3 we see the initial location of the melting layer (large UZh values) which gradually descends before it is below 1600 m at about 09:00 UTC. The corresponding Doppler velocity is shown in Fig. 4. The velocity shown here can be considered to be the effective terminal fall velocity of the hydrometeors. Effective, because updrafts and downdrafts may be both present depending on the meteorological situation. In the case of a stratiform rain event (a typical feature is the presence of a melting layer), the vertical velocity is expected on the scale of cm s^{-1} above the ML. The location of the melting layer is again nicely visible in the Doppler data. As soon there is a transition from snow into rain, terminal fall velocities increase

Radar observations of an orographic precipitation event

M. Frech and J. Steinert

[Title Page](#)

[Abstract](#)

[Introduction](#)

[Conclusions](#)

[References](#)

[Tables](#)

[Figures](#)

[⏪](#)

[⏩](#)

[◀](#)

[▶](#)

[Back](#)

[Close](#)

[Full Screen / Esc](#)

[Printer-friendly Version](#)

[Interactive Discussion](#)



does not have a correspondence to the fall velocities (Fig. 5). This appears indicative of small wet snow flakes. A substantial decrease of UZh to below 20 dBZ can be noted at about 17:00 UTC (Fig. 3) when surface observations report snowfall. Lower reflectivity factors suggest dry snow flakes. Note that the small ρ_{hv} values at higher elevations correspond to Zh values lower than 5 dBZ or less. Small ρ_{hv} values may occur because we are at the top of the precipitating cloud where the temporal variability of the scattering particles may be large.

With the help of the surface observations which indicate the transition into snow at 16:45 UTC, we can argue that the surface measurements between about 09:00 and 16:45 UTC are taken in the melting layer before we see the transition into snow. This needs to be kept in mind when interpreting the classification results.

We now investigate the corresponding surface observations. The time series of wind measurements based on an ultrasonic anemometer is shown in Fig. 6.

The whole event is characterized by a very constant wind direction. Wind speeds are on the order of 7 m s^{-1} , decreasing to about 5 m s^{-1} at about 14:00 UTC. Between 11:00 and 12:00 UTC there is no apparent change in wind speed and direction during the passage of the mesoscale feature observed in the radar data. In the case of a dynamic effect we may expect some evidence of horizontal divergence or convergence in the wind data. This can be a drop in wind speed or a change in wind direction. What we find however is a drop in surface pressure by about 1 hPa which is indicative of a dynamic effect even though it is not directly visible in the wind data. Possibly, lifting processes (eventually associated with the passage of a gravity wave), latent heat release and the capture of water droplets by snow lead to riming and generation of graupel or wet snow (Fabry and Zawadzki, 1995). Note, rain was still observed at the surface during the passage of this mesoscale event.

The corresponding observations of a Thies optical disdrometer are shown in Fig. 7. The optical disdrometer measures the hydrometeor size and fall speeds. Aside from precipitation rates a classification scheme based on the hydrometer sizes and fall speeds, together with a temperature measurement provides a diagnostic of the

HESSD

11, 8845–8877, 2014

Radar observations of an orographic precipitation event

M. Frech and J. Steinert

[Title Page](#)

[Abstract](#)

[Introduction](#)

[Conclusions](#)

[References](#)

[Tables](#)

[Figures](#)

[⏪](#)

[⏩](#)

[◀](#)

[▶](#)

[Back](#)

[Close](#)

[Full Screen / Esc](#)

[Printer-friendly Version](#)

[Interactive Discussion](#)



Radar observations of an orographic precipitation event

M. Frech and J. Steinert

[Title Page](#)

[Abstract](#)

[Introduction](#)

[Conclusions](#)

[References](#)

[Tables](#)

[Figures](#)



[Back](#)

[Close](#)

[Full Screen / Esc](#)

[Printer-friendly Version](#)

[Interactive Discussion](#)



hydrometeor type. The principal ideas and the caveats of such an instrument are discussed in e.g. Friedrich et al. (2013). During the passage of the mesoscale event there is a intensification of precipitation rate with an increase from 1 mm h^{-1} to on average 2 mm h^{-1} (Fig. 8). The relative contribution of the solid and liquid phase to the absolute precipitation rate does not reveal a link to the mesoscale precipitation event aloft. Nicely visible is the transition to snow fall in disdrometer data which corresponds very well to the observation of the weather observer (the ratio between solid QPE and total QPE becomes one). Timing and the transition corresponding to the sleet observation are well diagnosed by the disdrometer. Before that the liquid phase contribution is larger on average. Some of the variability of the ratio is related to small precipitation rates and the variability of the precipitation process itself where small variations in precipitation rates can lead to large fluctuations of the resulting precipitation ratio (Fig. 7).

4 Memmingen radar observations and hydrometeor classification

In the previous section we have analysed surface data and bird bath radar data at Hohenpeißenberg. Radar data show distinct mesoscale features which result in an increase in surface rain rate. The whole precipitation event is an example where the ML, initially nicely visible in the radar data (see early morning hours in Fig. 3), descends during the day. For a couple of hours the Hohenpeißenberg mountain top is actually within the ML before the surface observations indicate the transition into snow. We now use radar data from the operational Memmingen radar which is located 65 km West of Hohenpeißenberg. In the analysis we focus on the results of the hydrometeor classification. Aside from a correct HM classification we investigate the spatial HM variability which was visible from the birdbath scan. In the Hymec processing chain, the HM classification is used to select the appropriate quantitative precipitation algorithm. Before we go into detail it is necessary to point out the length and time scales involved when using in-situ measurements and radar measurements. With the main beam width of 1° , the radar pulse at a distance of 65 km has a width of about 1.1 km. The bottom

of the radar pulse at an elevation of 0.5° is at about 960 m as which corresponds approximately to the height of the Hohenpeißenberg. Recall that the range resolution is 1 km. The instantaneous radar measurement of this pulse volume is compared to an in-situ instrument which integrates over time (1 min). A perfect correspondence may only be expected if the meteorological phenomena is homogeneous in time and space for at least the time and length scales involved here. It is obvious that this will be only approximately the case here.

A PPI of the attenuation corrected Zh at the lowest elevation is shown in Fig. 9. It is taken at 11:50 UTC while the mesoscale event is passing the Hohenpeißenberg. The corresponding HM classification results are shown in Fig. 10. Based on the HM classification there is a gradient in snowfall height from North-West to South-East. This is highlighted by the fact that there is no circular melting layer “ring” around the radar. Instead, we find only a ring segment. This indicates a diabatic cooling effect associated with the synoptic scale warm front. During the persistent precipitation near the Alps, melting snow falling into the relatively warm airmass is causing diabatic cooling which leads to the continuous decrease of snowfall height (e.g. Lackmann et al., 2002, and references therein). The HM classification around the Hohenpeißenberg site predominantly shows wet snow associated with reflectivity factors on the order of 25 dBZ, consistent with the observation of the birdbath scan (Fig. 10). There are spots indicating rain with big drops which correspond to regions with enhanced Zh (Fig. 9). The Hohenpeißenberg weather observers still report rain during this time period. How can this be reconciled with the radar data? Obviously the scattering characteristics in the pulse volume is predominantly governed by the wet snow aloft, and not by the layer with rain close to the surface.

We will now compare a timeseries of HM classification based on the Memmingen radar with the standard HM classification of the optical disdrometer on the Hohenpeißenberg. The radar HM results are shown in Fig. 11 where the classification is shown as a time-height series based on volume data available every five minutes.

HESSD

11, 8845–8877, 2014

Radar observations of an orographic precipitation event

M. Frech and J. Steinert

[Title Page](#)

[Abstract](#)

[Introduction](#)

[Conclusions](#)

[References](#)

[Tables](#)

[Figures](#)



[Back](#)

[Close](#)

[Full Screen / Esc](#)

[Printer-friendly Version](#)

[Interactive Discussion](#)



HESSD

11, 8845–8877, 2014

Radar observations of an orographic precipitation event

M. Frech and J. Steinert

[Title Page](#)[Abstract](#)[Introduction](#)[Conclusions](#)[References](#)[Tables](#)[Figures](#)[⏪](#)[⏩](#)[◀](#)[▶](#)[Back](#)[Close](#)[Full Screen / Esc](#)[Printer-friendly Version](#)[Interactive Discussion](#)

The presented time span is between 06:00 and 20:00 UTC on 5 January 2013 and the height of HZEROCL and SNOWLMT are plotted together with the detected ML. The color table of the hydrometeor classes is the same as in Fig. 10. The melting layer can be seen until about 10:00 UTC which corresponds in timing and location quite well with melting layer height seen in Figs. 3 and 4. After about 10:00 UTC, wet snow is diagnosed in the lowest layer as the most likely HM type. A closer look on the classification results is given in Fig. 12. The HM classifications from the optical disdrometer are shown in Fig. 13.

The decrease of temperature on 5 January (Fig. 6) from approx. 4 °C at 00:00 UTC down to 0 °C around 17:00 UTC corresponds to the drop of the ML. The radar detected ML is shown in Fig. 14. The begin of the detected ML is around 02:00 UTC. Before this primarily rain and drizzle is diagnosed. In this example the detection of a ML ends around 10:00 UTC. As discussed before, the ML is at the height of the Hohenpeißenberg mountain. The Hymec result in Fig. 12 shows the change from melting layer to wet or dry snow after 10:00 UTC.

The classification of the disdrometer (Fig. 13) shows a mixture of drizzle or rain mixed with snow between 00:00 and 15:00 UTC. Then predominantly snow is seen which agrees well with the eye observations. However, before that the classification is not perfectly correct (the weather observers initially report rain, with a transition to sleet until 16:45 UTC). One may argue that the disdrometer HM algorithm also needs an optimization, but a “drizzle/rain with snow” class may be expected in ML.

During the time of rain and sleet observations (based on the weather observers) at the site until 16:45 UTC, the radar based HM detection predominantly sees wet snow as the prime HM. Considering the weather situation and the differences in sampling volume between the sensors used here we cannot say that the radar based HM classification is incorrect. It is consistent with what may be expected when measuring locally in a ML during an orographic rain event (recall that the depth of the ML can be on the order of several hundred meters), where, as discussed before, diabatic cooling is causing a temperature decrease so that snow may reach the ground even in an initially “warm”

airmass. From an operational point of view, the “correct” radar information should now be linked better to the surface observations. This may be achieved through improved training of the fuzzy logic scheme to better take into account the thermodynamic state of such a weather event, or by a statistical correction similar to a “model output statistics” (MOS) scheme (e.g. Glahn and Lowry, 1972). For this case study here, a significant adjustment of the MBF (which were taken from literature) seems not necessary. We also may conclude, that the temperature forecast by the model was sufficiently precise for this case.

5 Conclusions

An orographic precipitation event on 5/6 January 2013 is analyzed with respect to its temporal and spatial variability using polarimetric radar data. Radar data from the bird-bath scan together with disdrometer measurements at Hohenpeißenberg show the steady decrease of the melting layer in the course of the event until there is a transition into snow, which is indicated by the disdrometer measurements and confirmed by weather observers. The Hohenpeißenberg mountain top is in the ML for several hours. Radar measurements above the melting layer show mesoscale structures (length scale on the order of 25 km) that are interpreted as large wet snow because of the increased fall velocity on the order of 3 m s^{-1} . Associated surface observations show an increase in rain rate. Lifting processes (indicated by a drop in surface pressure) may be the cause for this.

A typical feature of an orographic precipitation event is, depending on the season, the transition from rain into snow due to diabatic cooling. This is a relevant meteorological situation for a weather service, which needs to be forecasted and detected by weather observing systems. Radar systems are the only devices that can provide a look into the precipitation process in high spatial and temporal resolution. With the introduction of new polarimetric radar systems a much better characterization of the hydrometeors is now possible. “Hymec” is DWD’s newly developed HM classifier which

HESSD

11, 8845–8877, 2014

Radar observations of an orographic precipitation event

M. Frech and J. Steinert

[Title Page](#)

[Abstract](#)

[Introduction](#)

[Conclusions](#)

[References](#)

[Tables](#)

[Figures](#)

[⏪](#)

[⏩](#)

[◀](#)

[▶](#)

[Back](#)

[Close](#)

[Full Screen / Esc](#)

[Printer-friendly Version](#)

[Interactive Discussion](#)



Radar observations of an orographic precipitation event

M. Frech and J. Steinert

[Title Page](#)

[Abstract](#)

[Introduction](#)

[Conclusions](#)

[References](#)

[Tables](#)

[Figures](#)

[⏪](#)

[⏩](#)

[◀](#)

[▶](#)

[Back](#)

[Close](#)

[Full Screen / Esc](#)

[Printer-friendly Version](#)

[Interactive Discussion](#)



is evaluated for this precipitation event. We use the Hymec results based on the volume and precipitation scan of the Memmingen radar which is situated 65 km away from Hohenpeißenberg. The Hymec detection of the melting layer height corresponds well with the radar observations of the birdbath scan. Once the ML is just above Hohenpeißenberg the HM are classified as wet snow with sporadic pockets of large rain drops, while there is still rain observed at the surface. Considering the size of the radar sensing volume and the fact that ML is above the radar site this is not considered as a incorrect Hymec classification. For this particular situation, either better thermodynamic input to Hymec or a statistical correction of the HM classification may help to better link the classification result to the surface observation. From an operational point of view of a weather service, this is the relevant “reference point”.

Overall Hymec performed well for this meteorological situation. A thorough validation of Hymec is underway. The results shown here are promising and indicate that the principle implementation has achieved a good level of quality considering the complexity of the precipitation phenomena.

The birdbath scan, which is usually used only for calibration purposes is a valuable source of information, as it provides a high resolution view of the precipitation process and dynamics above the radar site. It can reveal the corresponding variability in time and space. From an operational point of view it fits perfectly into DWD’s scan strategy where a volume scan is provided every 5 min. It can be viewed as an additional sweep of the volume scan.

Acknowledgements. The work of the Hohenpeißenberg weather observers is greatly acknowledged. The comments of Jörg Seltmann helped to improve this paper.

References

- Al-Sakka, H., Boumahmoud, A.-A., Fradon, B., Frasier, S. J., and Tabary, P.: A new fuzzy logic hydrometeor classification scheme applied to the French X-, C-, and S-band polarimetric radars, *J. Appl. Meteorol. Clim.*, 52, 2328–2344, 2013. 8849
- 5 Baldauf, M., Förstner, J., Klink, S., Reinhardt, T., Schraff, C., Seifert, A., and Stephan, K.: Kurze Beschreibung des Lokal-Modells Kurzzeitfrst COSMO-DE (LMK) und seiner Datenbanken auf dem Datenserver des DWD, Tech. rep., Deutscher Wetterdienst, Offenbach, Germany, 2014. 8850
- 10 Fabry, F. and Zawadzki, I.: Long-term radar observations of the melting layer of precipitation and their interpretation, *J. Atmos. Sci.*, 52, 838–851, 1995. 8854
- Frech, M.: Monitoring the data quality of the new polarimetric weather radar network of the German Meteorological Service, 36rd AMS Conference on Radar Meteorology, Breckenridge, CO, USA, 16 pp., 2013. 8847
- 15 Frech, M., Lange, B., Mammen, T., Seltmann, J., Morehead, C., and Rowan, J.: Influence of a radome on antenna performance, *J. Atmos. Ocean. Tech.*, 30, 313–324, 2013. 8847
- Frech, M., Seltmann, J., Hohmann, T., and Lang, P.: The Hohenpeißenberg polarimetric research radar: high resolution observations of a mesoscale convective system, *Meteorol. Z.*, in preparation, 2014. 8853
- 20 Friedrich, K., Higgins, S., Masters, F. J., and Lopez, C. R.: Articulating and stationary PARSIVAL disdrometer measurements in conditions with strong winds and heavy rainfall, *J. Atmos. Ocean. Tech.*, 30, 2063–2080, 2013. 8855
- Giangrande, S. E., Krause, J. M., and Ryzhkov, A. V.: Automatic designation of the melting layer with a polarimetric prototype of the WSR-88D radar, *J. Appl. Meteorol. Clim.*, 47, 1354–1364, 2008. 8850
- 25 Glahn, H. R. and Lowry, D. A.: The use of model output statistics (MOS) in objective weather forecasting, *J. Appl. Meteorol.*, 11, 1203–1211, 1972. 8858
- Keenan, T.: Hydrometeor classification with a C-band polarimetric radar, *Aust. Meteorol. Mag.*, 52, 23–31, 2003. 8849
- 30 Lackmann, G. M., Keeter, K., Lee, L. G., and Ek, M. B.: Model representation of freezing and melting precipitation: implications for winter weather forecasting, *Weather Forecast.*, 17, 1016–1033, 2002. 8847, 8856

Radar observations of an orographic precipitation event

M. Frech and J. Steinert

[Title Page](#)

[Abstract](#)

[Introduction](#)

[Conclusions](#)

[References](#)

[Tables](#)

[Figures](#)



[Back](#)

[Close](#)

[Full Screen / Esc](#)

[Printer-friendly Version](#)

[Interactive Discussion](#)



HESSD

11, 8845–8877, 2014

Radar observations of an orographic precipitation event

M. Frech and J. Steinert

Title Page

Abstract

Introduction

Conclusions

References

Tables

Figures



Back

Close

Full Screen / Esc

Printer-friendly Version

Interactive Discussion



- Lim, S., Chandrasekar, V., and Bringi, V. N.: Hydrometeor classification system using dual-polarization radar measurements: model improvements and in situ verification, *IEEE T. Geosci. Remote*, 43, 792–801, 2005. 8849
- 5 Park, H., Ryzhkov, A. V., Zrnić, D. S., and Kim, K.-E.: The hydrometeor classification algorithm for the polarimetric WSR-88D: description and application to an MCS, *Weather Forecast.*, 24, 730–748, 2009. 8849, 8851
- Rathmann, N. and Mott, M.: Effective radar algorithm software development at the DWD, 7th European Conference on Radar in Meteorology and Hydrology, NET316, available at: http://www.meteo.fr/cic/meetings/2012/ERAD/extended_abs/NET_316_ext_abs.pdf (last access: 28 July 2014), 2012. 8848
- 10 Scharfenberg, K. A., Schuur, T. J., Schlatter, P. T., Giangrande, S. E., Melnikov, V. M., Burgess, D. W., Jr., D. L. A., Foster, M. P., and Krause, J. M.: The Joint Polarization Experiment: polarimetric radar in forecasting and warning decision making, *Weather Forecast.*, 20, 775–788, 2005. 8847
- 15 Schuur, T. J., Park, H.-S., Ryzhkov, A. V., and Reeves, H. D.: Classification of precipitation types during transitional winter weather using the RUC model and polarimetric radar retrievals, *J. Appl. Meteorol. Clim.*, 51, 763–779, 2012. 8849
- Seltmann, J. E. E., Hohmann, T., and Frech, M.: DWD's new operational scan strategy, 36rd AMS Conference on Radar Meteorology, Breckenridge, CO, 2013.
- 20 Steinert, J., Werner, M., and Tracksdorf, P.: Hydrometeor classification and quantitative precipitation estimation from quality assured radar data for the DWD C-band weather radar network, 36th Conference on Radar Meteorology, 16–20 September 2013, Breckenridge, CO, USA, available at: https://ams.confex.com/ams/36Radar/webprogram/Handout/Paper228477/ams2013_poster363_steinert.pdf (last access: 28 July 2014), 2013. 8851
- 25 Straka, J. M., Zrnić, D. S., and Ryzhkov, A. V.: Bulk hydrometeor classification and quantification using polarimetric radar data: synthesis of relations, *J. Appl. Meteorol.*, 39, 1341–1372, 2000. 8849
- Werner, M. and Steinert, J.: New quality assurance algorithms for the DWD polarimetric C-band weather radar network, 7th European Conference on Radar in Meteorology and Hydrology, NET403, available at: http://www.meteo.fr/cic/meetings/2012/ERAD/extended_abs/NET_403_ext_abs.pdf (last access: 28 July 2014), 2012. 8850
- 30

Yuter, S. E., Kingsmill, D. E., Nance, L. B., and Löffler-Mang, M.: Observations of precipitation size and fall speed characteristics within coexisting rain and wet snow, *J. Appl. Meteorol. Clim.*, 45, 1450–1464, 2006. 8853

HESSD

11, 8845–8877, 2014

Radar observations of an orographic precipitation event

M. Frech and J. Steinert

[Title Page](#)

[Abstract](#)

[Introduction](#)

[Conclusions](#)

[References](#)

[Tables](#)

[Figures](#)



[Back](#)

[Close](#)

[Full Screen / Esc](#)

[Printer-friendly Version](#)

[Interactive Discussion](#)



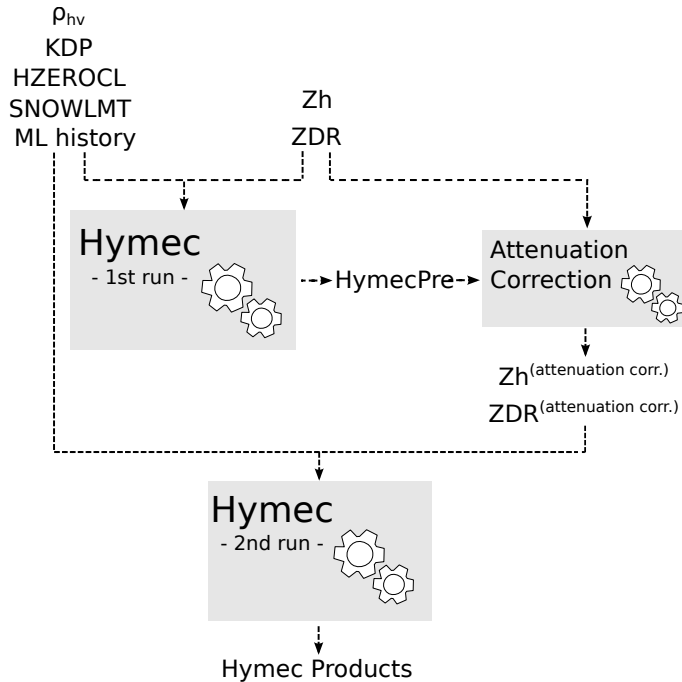


Figure 1. Structure of the two Hymec algorithm runs surrounding the attenuation correction. With dashed lines the data paths are displayed with the related data elements.

Radar observations of an orographic precipitation event

M. Frech and J. Steinert

[Title Page](#)

[Abstract](#)

[Introduction](#)

[Conclusions](#)

[References](#)

[Tables](#)

[Figures](#)

◀

▶

◀

▶

[Back](#)

[Close](#)

[Full Screen / Esc](#)

[Printer-friendly Version](#)

[Interactive Discussion](#)



Radar observations of an orographic precipitation event

M. Frech and J. Steinert

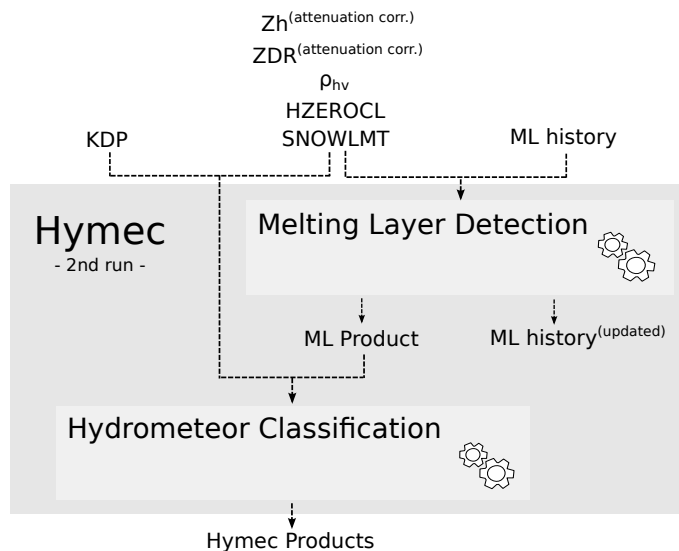


Figure 2. The inner structure of the 2nd run of the Hymec algorithm (see Fig. 1) including the melting layer detection and the hydrometeor classification. Presented are the used parameter and their data paths. This procedure is processed on every PPI sweep for each radar station separately.

[Title Page](#)
[Abstract](#)
[Introduction](#)
[Conclusions](#)
[References](#)
[Tables](#)
[Figures](#)
[◀](#)
[▶](#)
[◀](#)
[▶](#)
[Back](#)
[Close](#)
[Full Screen / Esc](#)
[Printer-friendly Version](#)
[Interactive Discussion](#)

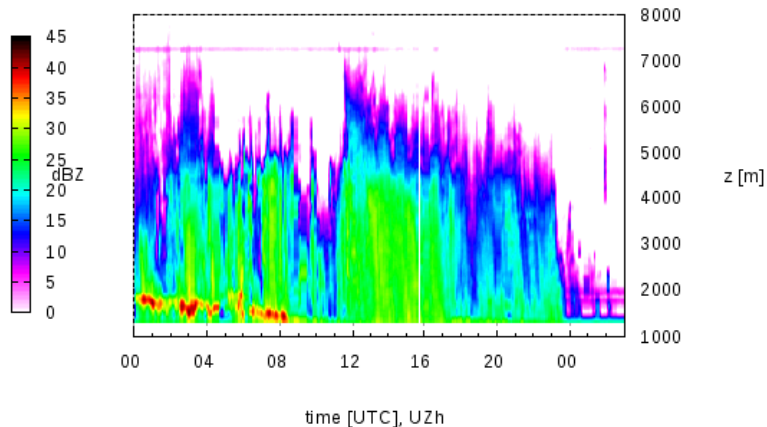



Figure 3. Time-height plot of UZh based on the birdbath scan which is available every 5 min. Data are from 5 January 2013 until 6 January 2013 in the morning, radar MHP.

Radar observations of an orographic precipitation event

M. Frech and J. Steinert

Title Page

Abstract

Introduction

Conclusions

References

Tables

Figures

◀

▶

◀

▶

Back

Close

Full Screen / Esc

Printer-friendly Version

Interactive Discussion



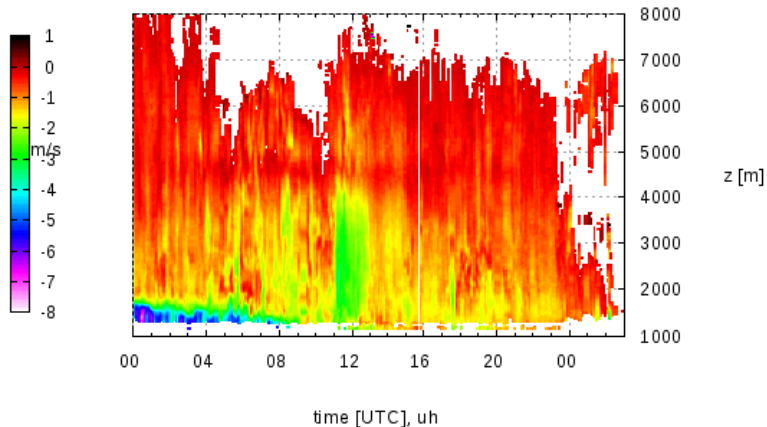


Figure 4. Time-height plot of Doppler velocity based on the birdbath scan which is available every 5 min. Data are from 5 January 2013 until 6 January 2013 in the morning, radar MHP. The data represents the effective terminal fall velocity of the hydrometeors (negative towards the surface).

Radar observations of an orographic precipitation event

M. Frech and J. Steinert

Title Page

Abstract

Introduction

Conclusions

References

Tables

Figures

◀

▶

◀

▶

Back

Close

Full Screen / Esc

Printer-friendly Version

Interactive Discussion

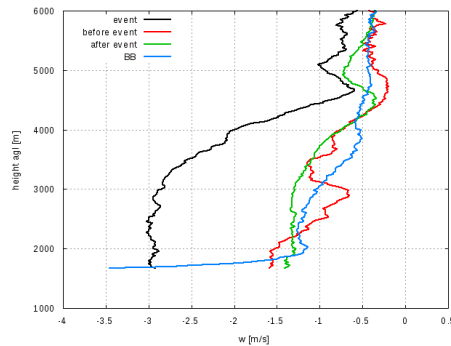
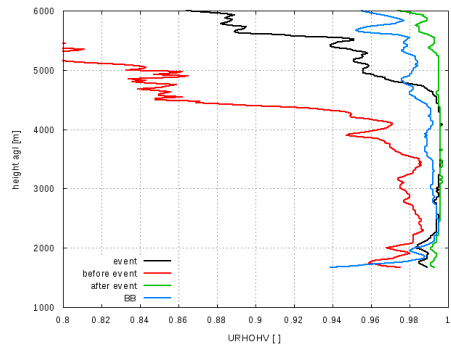
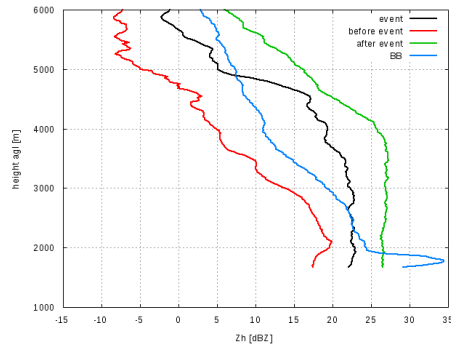


HESSD

11, 8845–8877, 2014

Radar observations of an orographic precipitation event

M. Frech and J. Steinert



Title Page

Abstract

Introduction

Conclusions

References

Tables

Figures



Back

Close

Full Screen / Esc

Printer-friendly Version

Interactive Discussion



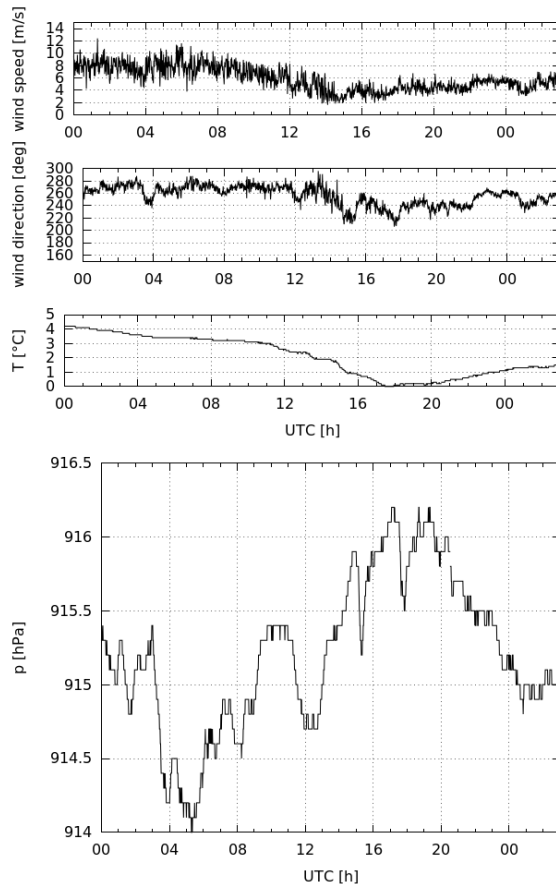


Figure 6. Time series of wind speed, wind direction (measured by a ultrasonic anemometer) and temperature (upper panel). Measurements are taken at the Hohenpeißenberg observatory. The corresponding surface pressure (hPa) is shown in the lower panel. Data start at 00:00 UTC, 5 January 2013 and end at 03:00 UTC, 6 January 2013.

Radar observations of an orographic precipitation event

M. Frech and J. Steinert

[Title Page](#)

[Abstract](#)

[Introduction](#)

[Conclusions](#)

[References](#)

[Tables](#)

[Figures](#)



[Back](#)

[Close](#)

[Full Screen / Esc](#)

[Printer-friendly Version](#)

[Interactive Discussion](#)



Radar observations of an orographic precipitation event

M. Frech and J. Steinert

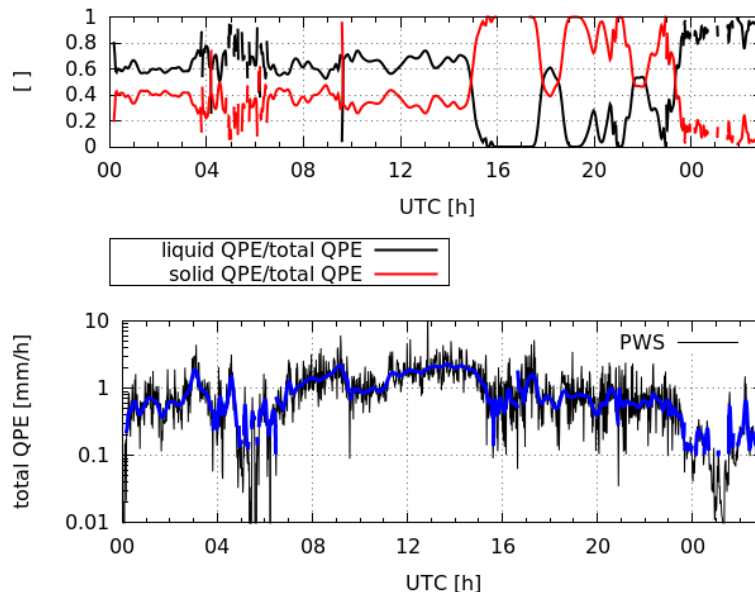


Figure 7. Raw and smoothed (in blue) timeseries of precipitation rate (mm h^{-1}) based on the Thies optical disdrometer (lower panel). The relative contribution of the liquid and solid phase precipitation to the total QPE (defined as the ratio of e.g. liquid QPE divided by the sum of liquid and solid QPE), upper panel. The ratio is only computed for precipitation rates larger than 0.1 mm. The resulting timeseries is then smoothed with a spline fit. Data shown begin at 00:00 UTC, 5 January 2013.

[Title Page](#)[Abstract](#)[Introduction](#)[Conclusions](#)[References](#)[Tables](#)[Figures](#)[⏪](#)[⏩](#)[◀](#)[▶](#)[Back](#)[Close](#)[Full Screen / Esc](#)[Printer-friendly Version](#)[Interactive Discussion](#)

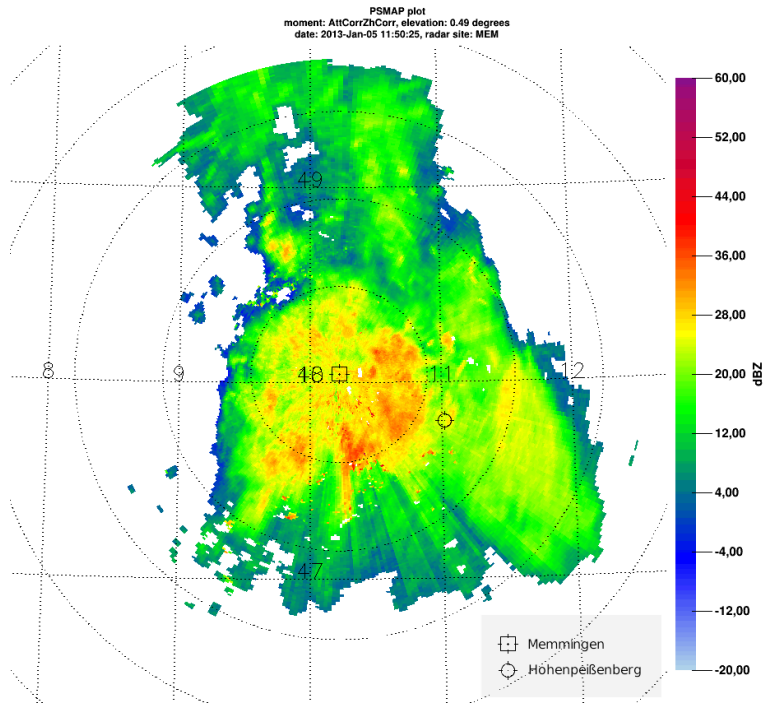


Figure 9. PPI of attenuation corrected Zh at an elevation of 0.5° for the Memmingen Radar at 11:50 UTC. The location of Hohenpeißenberg is indicated.

**Radar observations
of an orographic
precipitation event**

M. Frech and J. Steinert

Title Page

Abstract

Introduction

Conclusions

References

Tables

Figures

◀

▶

◀

▶

Back

Close

Full Screen / Esc

Printer-friendly Version

Interactive Discussion



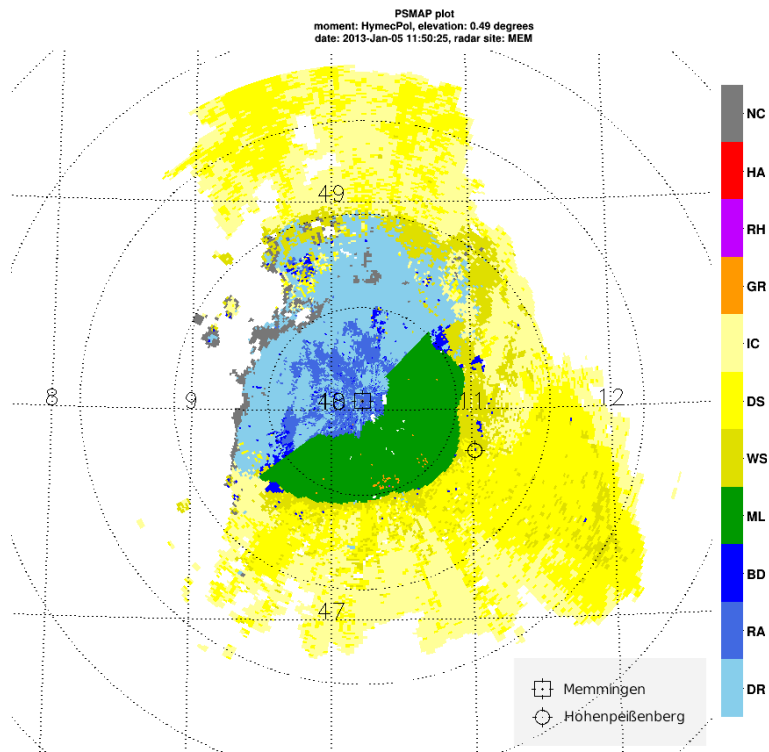


Figure 10. PPI of the hydrometeor classification at an elevation of 0.5° for the Memmingen Radar at 11:50 UTC. The location of Hohenpeißenberg is indicated. See text for an explanation of the various HM types.

Radar observations of an orographic precipitation event

M. Frech and J. Steinert

Title Page

Abstract

Introduction

Conclusions

References

Tables

Figures

⏪

⏩

◀

▶

Back

Close

Full Screen / Esc

Printer-friendly Version

Interactive Discussion



Radar observations of an orographic precipitation event

M. Frech and J. Steinert

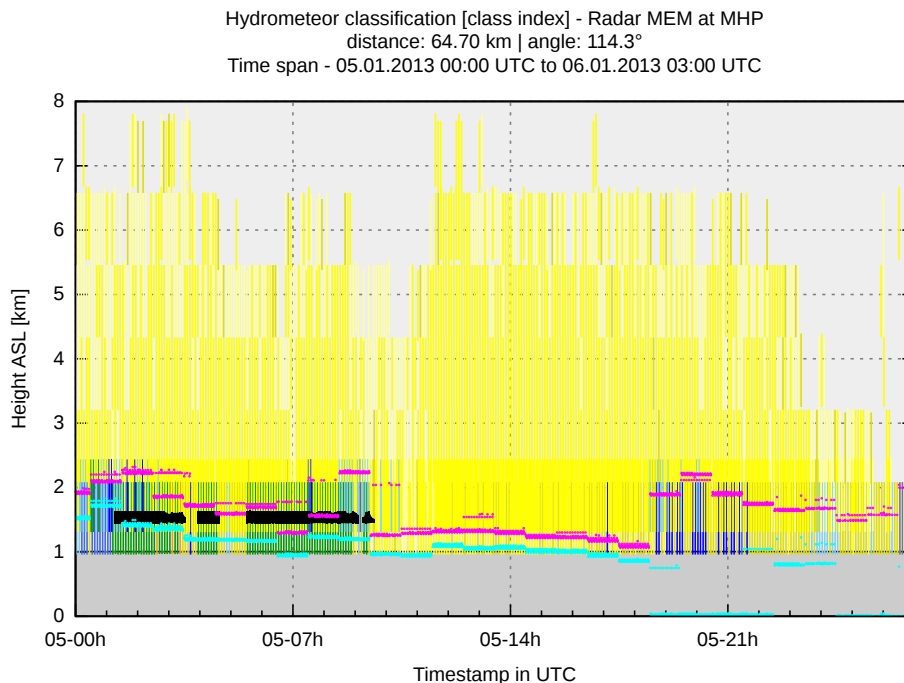


Figure 11. Time series of the hydrometeor classification for the precipitation scan and the volume scan of radar MEM at the position of MHP. Overlaid is the height of HZEROCL in magenta, the height of SNOWLMT in cyan and the melting layer history in black. The considered time span ranges from 00:00 UTC, 5 January 2013, until 03:00 UTC, 6 January 2013. The colour table for the hydrometeor classes is the same as in Fig. 10.

Title Page

Abstract

Introduction

Conclusions

References

Tables

Figures

◀

▶

◀

▶

Back

Close

Full Screen / Esc

Printer-friendly Version

Interactive Discussion



Radar observations of an orographic precipitation event

M. Frech and J. Steinert

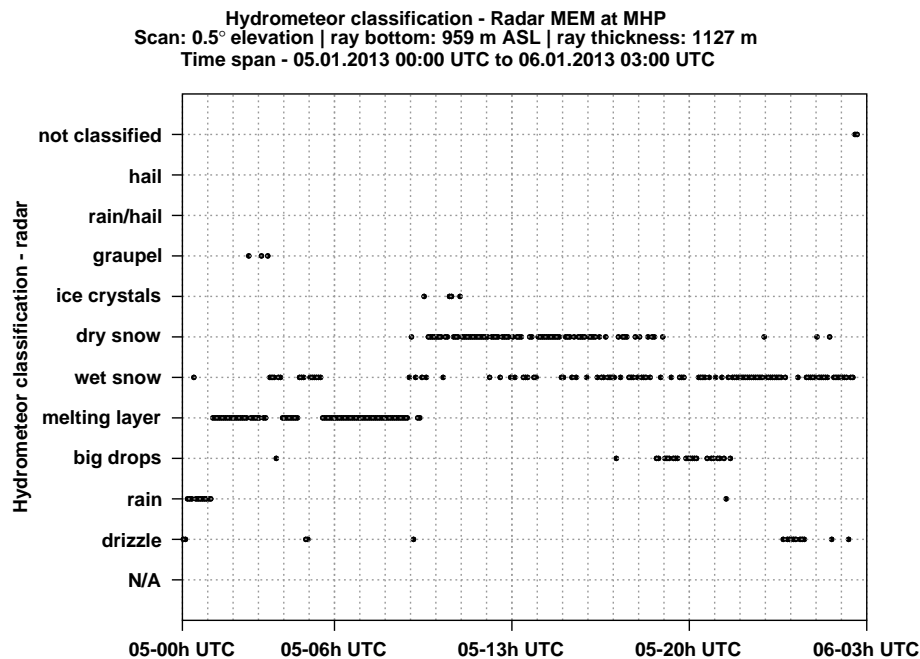


Figure 12. Time series of the hydrometeor classification for the 0.5° elevation volume sweep of radar MEM at the position of MHP. At this location the radar ray has a mean vertical extension of 1127 m and the height of the ray bottom is estimated with 959 m a.s.l. Displayed are the distinct hydrometeor classes with the highest detection probability.

Title Page

Abstract

Introduction

Conclusions

References

Tables

Figures



Back

Close

Full Screen / Esc

Printer-friendly Version

Interactive Discussion



Radar observations of an orographic precipitation event

M. Frech and J. Steinert

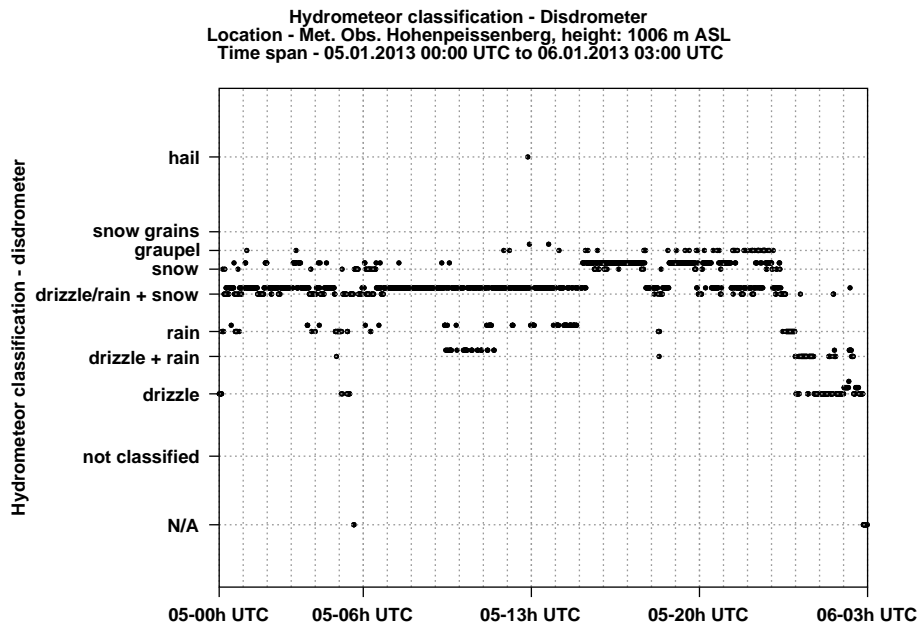


Figure 13. Time series of the hydrometeor classification from Thies disdrometer, located at MHP. The hydrometeor classes are based on the synoptic classification related to table 4680. Mixtures of classes are denoted as combination of the distinct classes. The class labels are related to the lowest intensity. Higher intensities are displayed by data points slightly above the related label.

[Title Page](#)
[Abstract](#)
[Introduction](#)
[Conclusions](#)
[References](#)
[Tables](#)
[Figures](#)

[Back](#)
[Close](#)
[Full Screen / Esc](#)
[Printer-friendly Version](#)
[Interactive Discussion](#)


Radar observations of an orographic precipitation event

M. Frech and J. Steinert

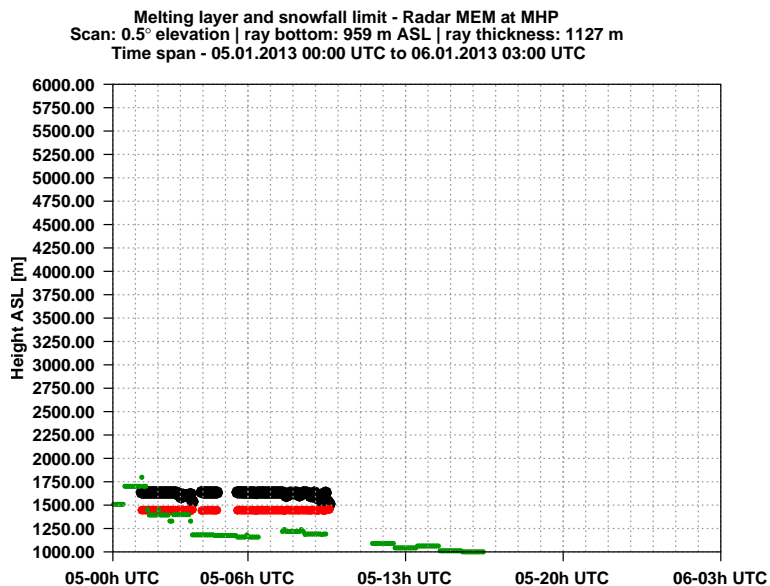


Figure 14. Time series of the detected melting layer for the radar data of MEM at the position of MHP. The ML is represented by the upper limit (black) and the lower limit (red). For comparison the estimated snowfall height (COSMO-DE model output) is drawn in green.

[Title Page](#)[Abstract](#)[Introduction](#)[Conclusions](#)[References](#)[Tables](#)[Figures](#)[◀](#)[▶](#)[◀](#)[▶](#)[Back](#)[Close](#)[Full Screen / Esc](#)[Printer-friendly Version](#)[Interactive Discussion](#)